IEEE Access
Multidisciplinary | Rapid Review | Open Access Journal

Received June 26, 2021, accepted July 26, 2021, date of publication August 9, 2021, date of current version August 13, 2021.

Digital Object Identifier 10.1109/ACCESS.2021.3103243

W-Band Sensor for Complex Permittivity Measurements of Rod Shaped Samples

YEVHEN YASHCHYSHYN[1,3], (Senior Member, IEEE), KRZYSZTOF DERZAKOWSKI[1], CHANGYING WU[2], (Member, IEEE), AND GRZEGORZ CYWIŃSKI[3,4]

[1]Institute of Radioelectronics and Multimedia Technology, Warsaw University of Technology, 00-665 Warsaw, Poland
[2]School of Electronics and Information, Northwestern Polytechnical University, Xi'an 710072, China
[3]CENTERA Laboratories, Institute of High Pressure Physics, Polish Academy of Sciences, 01-142 Warsaw, Poland
[4]CEZAMAT, Warsaw University of Technology, 02-822 Warsaw, Poland

Corresponding author: Krzysztof Derzakowski (krzysztof.derzakowski@pw.edu.pl)

This work was supported in part by the CENTERA Laboratories in the framework of the International Research Agendas Program through the Foundation for Polish Sciences by the European Union by the European Regional Development Fund under Grant MAB/2018/9.

ABSTRACT A novel W-band sensor for complex permittivity measurements of rod shaped samples based on reflectometer method is described. Characterization of dielectric materials around 100 GHz is quite a challenge. The main limitation is the requirements for the accuracy of the dimensions of the test sample and ensuring good contact with conductive surfaces. From this point of view, it seems interesting to use a cylindrical waveguide with the TE_{01} mode. The four linearly-polarized H_{10} fields of rectangular waveguides with equal amplitude and phase circumnavigate the cylindrical waveguide to jointly excite its TE_{nm} circular modes with four-fold symmetry. This precludes the excitation of lower-order modes of the metallic cylindrical waveguide. TE_{01} mode is unique in that its field leads to zero on the surface of the walls of a metallic cylindrical waveguide. The main field interaction takes place on the sample surface. The calibration method uses calibration curves obtained by simulation for known values of complex permittivity of the samples. This eliminates the requirement for a precision calibration standards, which is the problematic to realize at millimeter wavelengths. Moreover, the complex field structure in the sensor makes it impossible to apply a standard calibration method. Simulation and measurements using these method have been performed in W-band (70-114 GHz). Measurement results demonstrate the robustness of this new sensor for characterizing rod shaped dielectric samples.

INDEX TERMS Dielectric materials, dielectric measurement, microwave and millimeter wave measurements, microwave sensors, reflectometry.

I. INTRODUCTION

The W band of the electromagnetic spectrum ranges from 75 to 110 GHz is used for satellite communications, millimeter-wave automotive cruise control radar, military radar targeting and tracking applications, and some non-military applications. An interesting application of this frequency range is the heating effect. Less-than-lethal weaponry exists that uses millimeter waves to heat a thin layer of human skin to an intolerable temperature so as to make the targeted person move away. A two-second burst of the 95 GHz focused beam heats the skin to a temperature of 130 F (54 °C) at a depth of 1/64 of an inch (0.4 mm). The United States Air Force and Marines are currently using this type of Active Denial System [1]. The use of various dielectric materials to protect against radiation or ensuring the correct operation of the devices being developed requires knowledge of their characteristics. In any case, determining the permittivity of materials in W band is very timely.

The applied methods of measuring material parameters in the microwave frequency range depends on several parameters, such as the frequency, size and shape of the available samples, the extent of dielectric losses and the presence of anisotropy [2]. Generally, these methods can be divided into transmission/reflection [3]–[5] and resonator methods. For transmission/reflection methods, the transmission coefficient or reflectance is measured. Transmission/reflection measurements can be performed using a closed measurement structure, e.g. coaxial lines, waveguides, as well as open ended probes, and can also be carried out in free space [6], [7]. These methods are useful, first of all, in the case of measuring the permittivity of a small value, of the order of several, and for

The associate editor coordinating the review of this manuscript and approving it for publication was Mira Naftaly.

high loss and medium loss samples. These ones can be used for frequencies below 10 GHz due to the significant increase in loss above this frequency. The exception is free space measurement methods that can be used at higher frequencies. Uncertainties for real permittivity is better than ±1%. Resolution of loss tangent measurements is limited (typically ±0.01).

Resonator methods can be divided into two groups: metal cavity [8]–[10] and dielectric resonator method [11]–[13]. These methods also include the Fabry-Perot resonator method [14]–[16]. Generally, the resonant frequency and the unloaded Q-factor of a cavity resonator with a sample of the material under test or of a resonator formed by the sample itself, the so-called dielectric resonator are measured. On the base of this measurement, the permittivity and loss tangent is extracted.

Among the methods with a cavity resonator, the most frequently used are waveguide cavities working with first of TE_{01n} or TM_{01n} modes. One of the main advantages of the TE_{01n} modes methods is that it is insensitive to air gaps between the symmetrically placed sample and the cavity resonator. It is related to the field distribution in the cavity. The accuracy of the measurement depends largely on the losses in the tested sample. For very small losses, the accuracy decreases due to the large proportion of losses in the metal walls of the resonator. Another disadvantage is that for frequencies below 8 GHz, the resonator sizes become large. Uncertainties of real permittivity determination employing TE_{01n} mode cavities are the order of 0.5%. In the TM_{01n} mode resonators, samples filling the entire cavity depth are used. Unfortunately, such a solution is very sensitive to air gaps between the sample and the structure. Typical measurement uncertainties for real permittivity are about 0.5%–2%. Fabry–Perot resonators are commonly used in the mm-wave range for low-loss materials. The achieved accuracy of the measurement of the real part of the permittivity is about 0.5%. The disadvantage is the need to make the resonator accurately and the large size of the sample.

In the methods with the dielectric resonator, the fact that almost 90% of the electromagnetic field energy is concentrated in the measured sample is used. Different modes and different structures are used [11]–[13]. The resonant frequency of the dominant modes as well as the higher modes, e.g. the whispering gallery modes, is determined. The limitation in the use of methods with the basic mode is its size, because in order for the dielectric resonator to be a good resonator, it must have high permeability, which reduces its size and limits its use to about 20 GHz. Another limitation is the amount of material losses - the best results are obtained for small and very small values of the loss tangent. The achievable accuracy is 10^{-6} for the loss tangent of materials with high permeability ($\varepsilon > 20$) and 0.3% for the measurement of the real part of the permeability - regardless of their value. For higher frequencies it is possible to use whispering gallery resonators. The main advantage of the whispering gallery methods is the almost unlimited resolution of the loss tangent measurement, unfortunately only for losses less than 10^{-4}. Another disadvantage of these methods is the difficulty in correctly determining the mode.

Characterization of dielectric materials at frequencies around 100 GHz is quite a challenge. The main limitations are the requirements for the accuracy of the dimensions of the test sample and ensuring good contact with conductive surfaces. From this point of view, it seems interesting to use a cylindrical waveguide with the TE_{01} circular (called TE_{01}cir.) mode. TE_{01}cir. mode is unique in that its field leads to zero on the surface of the walls of a metallic cylindrical waveguide because exciting only E_{φ} component. An example of the way to excite the TE_{01}cir. mode is shown in [17]. The four linearly-polarized H_{10}reg. fields of rectangular waveguides with equal amplitude and phase circumnavigate the cylindrical waveguide to jointly excite its TE_{nm} circular modes four-fold symmetry. This precludes the excitation of lower-order modes of the metallic cylindrical waveguide (i.e., TE_{11}cir., TM_{01}cir. TE_{21}cir., TM_{11}cir.). It will be the best, but the bandwidth of spectral characteristics of the mode converter form H_{10}reg. to the TE_{01}cir. is about 5% only. If you want to use the whole W-band then we cannot work with TE_{01}cir modes only. In [18] a generic approach to excite a pure circular TE_{mn}cir mode through sidewall couplings with the emphasis on the coupling mechanism is presented. Particular attention was paid to the analysis of the modes excited by the converter. Three mode converters TE_{21}cir, TE_{01}cir, TE_{41}cir, were designed, built, and tested at W-band (75 – 110 GHz). It has been shown that the measurements of back-to-back transmission show the maximum transmission bandwidth of 24 GHz for the TE_{01}cir converter.

II. SENSOR DESIGN AND DATA PROCESSING TECHNIQUES

In this work, we consider the use of a similar converter in order to apply it to the characterization of a dielectric sample that is introduced inside a cylindrical waveguide in which the TE_{mn} mode is excited. The converter dimensions were selected by means of preliminary simulations: quad feed by WR-10 rectangular waveguides (2.54 × 1.57 mm), radius of a cylindrical waveguide is equals 1.75 mm. The Fig. 1 shows the model of designed sensor. The sensor consists of two identical parts connected together. Fig.1.b) shows one of these parts, which are tightly joined with pins and screws. Each parts made of brass and machined using a computer numerically controlled (CNC) lathe with a tolerance of 5 μm.

In Fig. 2 green and yellow colors represent metal, blue - Teflon, purple – sample. The sample height equal to 2.5 mm, diameter equal to 1.5 mm. The shape of the sample indicates that the sensor can be used for characterizing the samples in the form of a cylinder. This is a very important aspect when industrial materials are present or when samples are prepared in the form of rods, which is easier than other forms. Small holes in the metal part (yellow in color) will allow the use of such a sensor for testing liquids in the future. The choice of the conical shape of the metal parts is related to

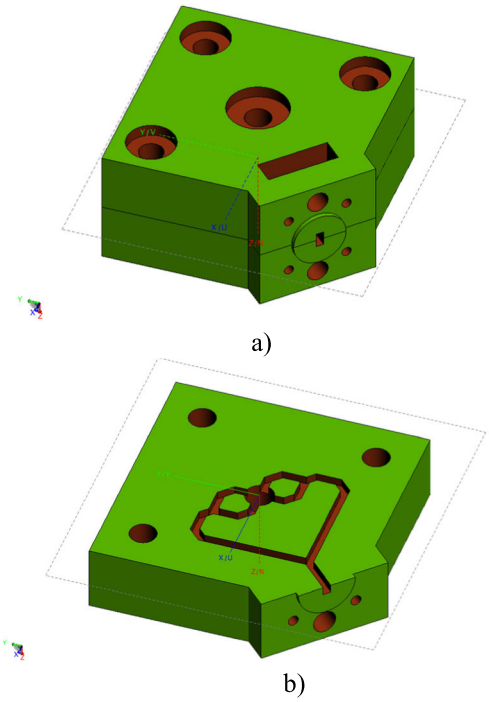

FIGURE 1. Model of sensor prepared for fabrication (a), one of two parts of the sensor (b).

the need to gently clamp the sample, which is placed in a Teflon holder with a diameter equal to 3.5 mm. As it was mentioned that TE_{01}cir. mode is unique in that its field leads to zero on the surface of the walls of a metallic cylindrical waveguide because exciting only E_φ component. The main field interaction takes place on the sample surface.

The mathematical model includes a metallic circular waveguide of inner radius r_t, inner wall of which is containing a Teflon lining of inner radius r_d and relative permittivity ε_t for the full length of the waveguide [19]. The model includes a coaxial dielectric insert of radius r_d and relative permittivity ε_d which can be changed, Fig. 3.

The structure may be divided into two analytical regions, the central dielectric filled region I: $0 \le r \le r_d$ and the Teflon filled region II: $r_d \le r \le r_t$. For TE_{01} mode we can write (1):

$$\gamma^{II} J_0'\{\gamma^I r_d\}(J_0\{\gamma^{II} r_d\}Y_0'\{\gamma^{II} r_t\} - Y_0\{\gamma^{II} r_d\}J_0'\{\gamma^{II} r_t\}) = \gamma^I J_0\{\gamma^I r_d\}(J_0'\{\gamma^{II} r_d\}Y_0'\{\gamma^{II} r_t\} - Y_0'\{\gamma^{II} r_d\}J_0'\{\gamma^{II} r_t\}) \quad (1)$$

where J_0 and Y_0 are the zeroth-order Bessel functions of the first and second kinds, respectively. Prime with a function represents the derivative with respect to its argument; $\gamma_n^I = \sqrt{(\varepsilon_d k^2 - \beta_n^2)}$ and $\gamma_n^{II} = \sqrt{(\varepsilon_t k^2 - \beta_n^2)}$ are radial propagation constants in regions I and II, respectively. k and β_n are the free space and phase propagation constants.

The results of calculation of the radial propagation constant depend on the frequencies and permittivity of samples is shown in Fig. 4.

The propagation constant depend on the permittivity of samples for three frequencies is shown in Fig. 5

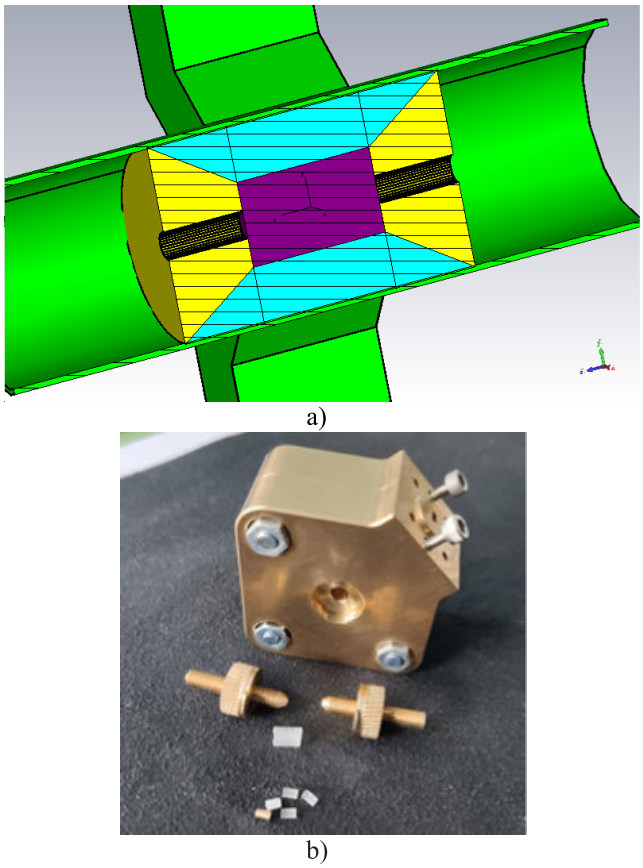

FIGURE 2. The longitudinal cross-section of a sensor a) and fabricated sensor with accessories and samples (b).

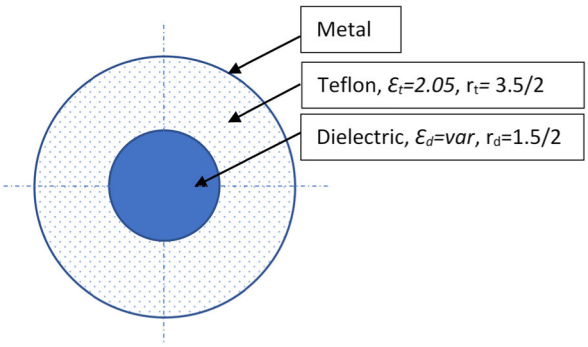

FIGURE 3. The model of cylindrical coaxial waveguide.

Form obtained results we can say that it possible extract some information connected with permittivity of sample under test. However, the extraction is not possible with using well known algorithms and advanced calibration methods. Therefore we propose a different approach.

The calibration method uses calibration curves obtained by simulation for known values of complex permittivity of the samples. This eliminates the requirement for a precision calibration standards, which is the problematic to realize at millimeter wavelengths. Moreover, the complex field structure in the sensor makes it impossible to apply a standard calibration method. Simulation and measurements using these method have been performed in W-band (70-114 GHz). The sensor

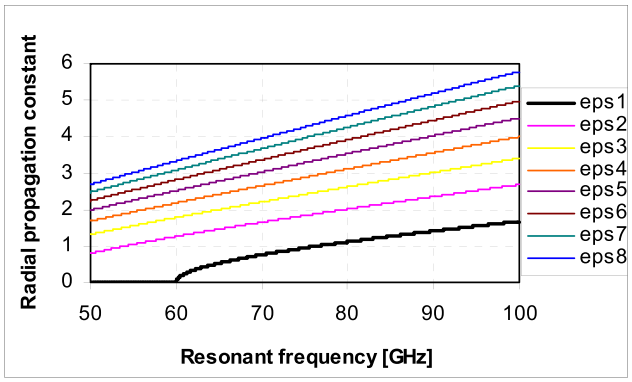

FIGURE 4. The radial propagation constant γ_1 as a function of a frequency.

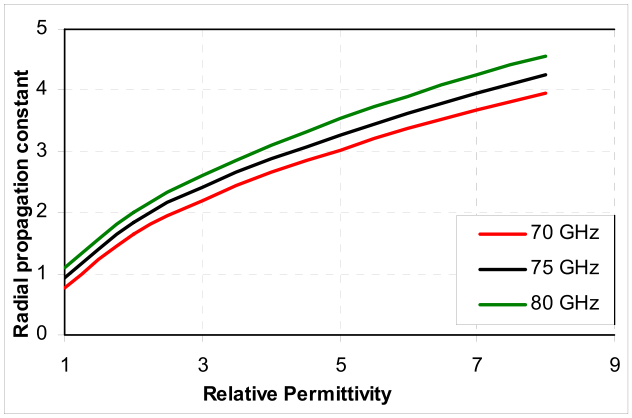

FIGURE 5. The radial propagation constant γ_1 as a function of relative permittivity.

was used to measure the complex reflection coefficient in a W-band depending on the relative permittivity ε_i of the sample under test.

$$S_{11}(f, \varepsilon_i) = |S_{11}(f, \varepsilon_i)| \cdot exp\{j \cdot phase(S_{11}(f, \varepsilon_i))\} \quad (2)$$

The sensor was not a special matched due to the fact that introducing material under test will cause the sensor unmatched. Calibration was performed only on the waveguide input of the sensor. The complex reflection coefficient contains information about the amplitude and phase of the wave reflected from the sample. At the beginning we will use phase dependencies, which are processed in this way: measured unwrapped values of the phase for the samples are normalized by the air sample unwrapped phase value. After normalization, the mean values for each sample were calculated:

$$diff(phase) = \frac{1}{N}\sum_{n=1}^{N} \times \{phase[S_{11}(f_n, \varepsilon_i)] - phase[S_{11}(f_n, \varepsilon_A)]\} \quad (3)$$

where N – number of frequency points in chosen frequency band; *phase* - the phase angle in the interval $[-\pi, \pi]$ for each element of a complex reflection coefficient S_{11}; $S_{11}(f_n, \varepsilon_A)$ – reflection coefficient for empty sample.

Based on the mean phase difference values, it was possible to determine dependence on the permittivity of the samples.

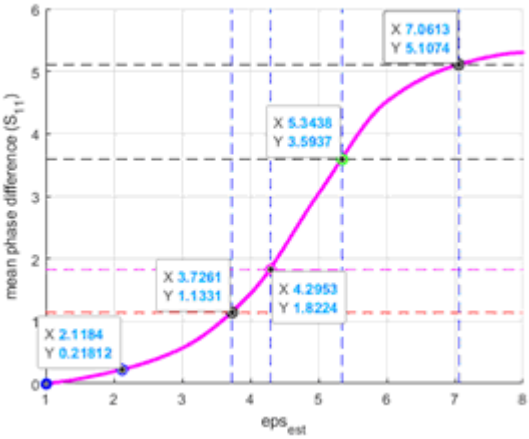

FIGURE 6. Dependence for relative permittivity equal to 2.05 (Teflon), 4.826, 6.567 and 7.878 on the mean phase difference.

However, the problem is sensor calibration, which is not easy or impossible to perform. In this study, it was proposed to use the calibration curve obtained on the basis of simulations carried out in the CST simulator. The calibration curve is the result of calculation the simulated mean phase different values for known permittivities (Fig. 6). The calibration curve is constructed using the following sample permittivity values in the frequency band from 70.5 GHz to 79 GHz: 1 (Air), 2.05 (Teflon), 3, 3.75 (Quartz), 4, 4.5, 5, 5.5, 6, 7 and 8. The influence of the frequency band on the shape of the calibration curve depends on the selected bandwidth and will be analyzed in the following part of the work. Calibration curve now makes it possible to easily determine the permittivity of the samples under test. The mean values of phase difference after normalization, for example for $Quartz_M$ is 1.1492 and is shown in Fig. 6 by a horizontal dotted red line. The point where this red line intersects with the calibration curve shows us the relative permittivity for $Quartz_M$ which is equal to 3.75, exactly as much as the sample in the simulation. The designation $Quartz_M$ and Quartz determines the amount of permittivity measured and obtained by simulation for the Quartz sample. Except of the samples mentioned above (Teflon and $Quartz_M$), with relatively known parameters, were used for testing specially prepared materials (Fig. 7) with different permittivity around "4" (sample no 4), "6" (sample no 6) and "8" (sample no 8), respectively.

The main advantage of such a material is that it can be slightly shaped at a temperature of around 40 degrees, supposedly like using plasticine. Obtaining the appropriate permittivity is achieved by introducing a certain percentage of TiO_2. Relative permittivity values were obtained in X-band using the resonant method, called the split post dielectric resonator method [20].

The sample with thin plate shape was placed between two parts of cylindrical dielectric resonator. The mean values of the real permittivity of the samples and tan δ were taken: "4" = 4.826 × 0.00347; "6" = 6.567 × 0.004153; "8" = 7.878 × 0.0047725. In the W-band, the use of the resonance method is not possible due to the requirement of too

FIGURE 7. The specially prepared materials with different permittivity.

small dimensions of test samples. In the W-band, the results obtained by the proposed method are as follows: sample "4" gives a permittivity of 4.2054; sample "6"–5.1341; sample '8'–6.8916 (Fig.3). The obtained values of the permittivity of the samples at W-band are slightly lower than it is known in literatures, which may agree with the behavior of dielectrics at higher frequencies, comparing permittivity in the X- and W-band. The use of other samples was not possible due to their absence and the lack of information on their permittivity in the W-band.

Using the designed sensor, it is also possible to estimate the losses on the basis of the amplitude relation of reflection coefficient. Apparently, as for the phase, the amplitude is normalized to the reflection amplitude for a metal sample. So, the power dissipated (losses) in samples can be estimated (4).

Knowing the dissipated power one can calculate the dissipation factor (3) or well known as a tan δ (5).

$$losses\,(\varepsilon_i) = 1 - \frac{1}{N}\sum_{n=1}^{N}\left\{\left|S_{11}\,(f_n, \varepsilon_i)\,/S_{11}\,(f_n, \varepsilon_M)\right|^2\right\} \quad (4)$$

where $S_{11}\,(f_n, \varepsilon_M)$ – reflection coefficient for metal sample.

$$tan\,(\delta) = \left\{\frac{losses\,(\varepsilon_i)}{\sqrt{1 = losses\,(\varepsilon_i)}} - tan\,(\delta_A)\right\} / \left[2real\varepsilon_i\right] \quad (5)$$

The results of processing the dissipated power are shown in Fig. 8. Colored solid curves show simulated different levels of tan δ: blue – 0.0005, violet – 0.001, black – 0.005, and red – 0.01. The results obtained on the basis of the measurement are shown by means of separate colored circles.

The designation Quartz_M and Quartz determines the amount of permittivity measured and obtained by simulation for the Quartz sample. The results clearly show that the applied method significantly increases the accuracy of the tan δ estimation. As a result, it can be concluded that the obtained results for Teflon and Quartz are very similar. For Teflon in simulation tanδ was assumed to be 0.0003, Quartz – 0.0004. As a result of the tan δ measurements for the Quartz_M, it is equal to 0.0009, for the Teflon_M tanδ = 0.0005. For the samples "4", "6" and "8" tanδ is close to 0.01. It can be stated that for samples "4" tanδ = 0.008; for "6" tanδ = 0.0055, and for sample "8" – 0.012. The obtained values of the tan δ of the samples in W-band are higher compare to results obtained in X-band, which may agree with the behavior of dielectrics at higher frequencies. Measurement results demonstrate the robustness of this new sensor for characterizing rod.

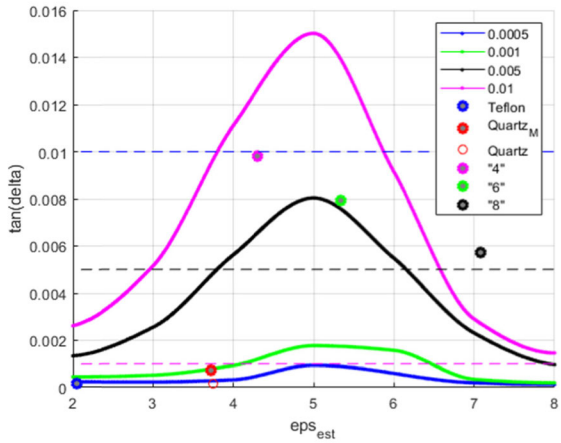

FIGURE 8. Dependence of losses on relative permittivity.

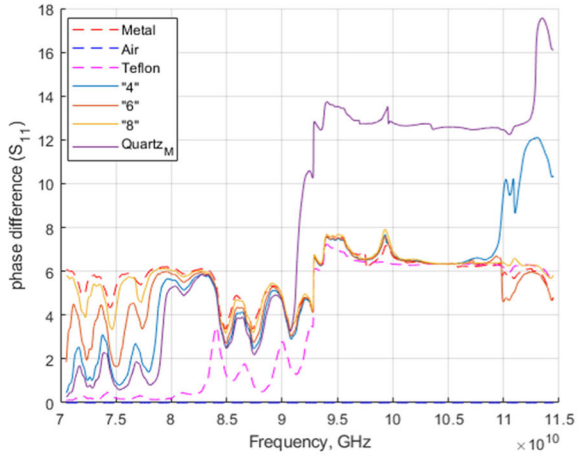

FIGURE 9. Processed measured phase difference of reflection coefficients vs W-band frequency for different samples.

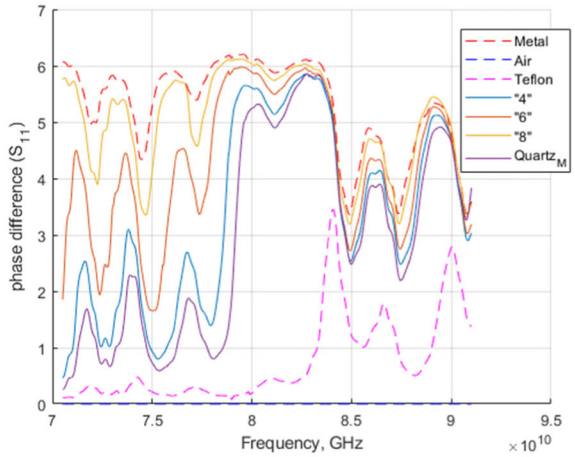

FIGURE 10. Processed measured phase difference of reflection coefficients in frequency band from 70.5 GHz to 91 GHz.

TABLE 1. Results of measurement.

Sample	Thickness [mm]	Air gap [mm]	Resonant frequency [GHz]	Q-factor	Permittivity	Loss tangent x 10^{-3}
"4"	1.8	0.00	9.830025	1394.330	4.815239	4.62
"4"	1.8	0.02	9.899700	1859.099	4.852851	3.32
"4"	1.5	0.00	9.790275	2175.617	4.870999	2.90
"4"	1.5	0.01	9.842175	2187.150	4.764605	3.03
"4"	**2.5xΦ1.5**		**W-band**		**4.3**	**8**
"6"	1.8	0.00	9.606525	707.663	6.489368	6.81
"6"	1.8	0.01	9.638850	1127.351	6.557295	4.05
"6"	1.8	0.02	9.674475	1482.678	6.588322	2.95
"6"	1.8	0.03	9.706500	1559.277	6.632488	2.80
"6"	**2.5xΦ1.5**		**W-band**		**5.34**	**5**
"8"	1.98	0.00	9.407850	685.454	7.805609	5.26
"8"	1.98	0.01	9.443775	753.994	7.852244	4.76
"8"	1.98	0.02	9.475725	804.732	7.911845	4.44
"8"	1.98	0.03	9.510225	777.933	7.941921	4.63
"8"	**2.5xΦ1.5**		**W-band**		**7.06**	**12**
$Quartz_M$	**2.5xΦ1.5**		**W-band**		**3.73**	**0.7**
$Teflon_M$	**2.5xΦ1.5**		**W-band**		**2.12**	**0.3**

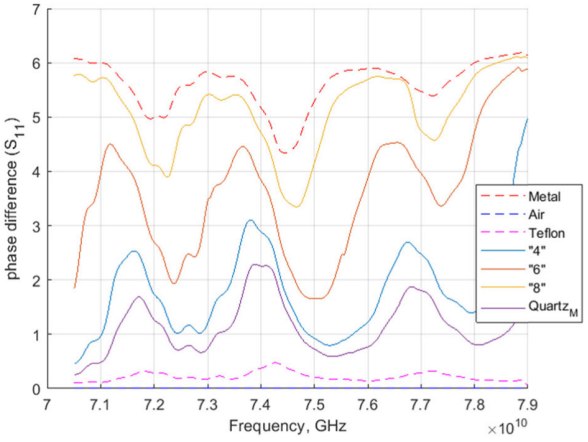

FIGURE 11. Processed measured phase difference of reflection coefficients frequency band from 70.5 GHz to 79 GHz.

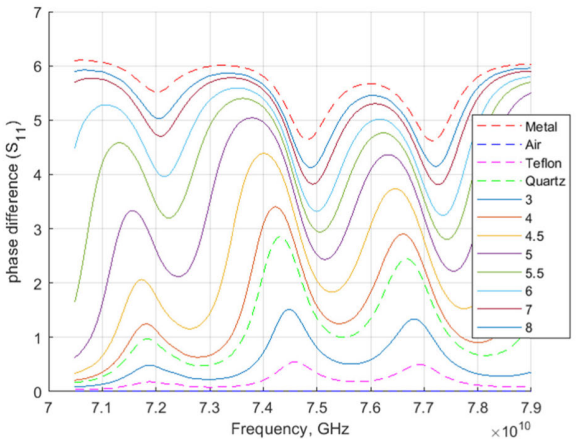

FIGURE 12. Processed simulated phase difference of reflection coefficients vs frequency for different samples with known permittivities.

III. EFFECT OF BANDWIDTH ON THE SENSOR CHARACTERISTICS

The correct operation of the sensor depends on the correctly selected operating bandwidth. Fig. 9 shows the measured and processed phase difference of the reflection coefficient relationship in the W-band for several different samples under test. It is very easy to notice four frequency bands in which phase changes are visible depending on the permittivity of sample: 1) 70.5 GHz-79 GHz; 2) 80 GHz-93 GHz 3) 93 GHz-110 GHz and 4) above 110 GHz. These bands are associated with the different types of modes that excite in the sensor. The most interesting in our case is the first range that corresponds to the TE_{01}cir. mode. Figures 10 and 11 show in detail the dependence of the phase change on the permittivity of the sample in the second and first frequency ranges.

Moreover, in Fig. 12 the simulation results carried out in the CST simulator for a first range of frequency are shown which are comparable to the results shown in Fig. 11. On the basis of these simulations a calibration curve is built (Fig. 6).

IV. CONCLUSION

The using calibration curves obtained by simulation for known values of complex permittivity of the samples is very promising. The possibilities of obtaining calibration curves for real part of permittivity and for tan δ are shown. The results clearly show that the applied method significantly increases the accuracy of the tan δ estimation. Teflon and Quartz samples were used to compare the quality of the samples due to their known permittivity. Other artificially prepared samples (due to the possibility of changing their shape) were characterized using the very well-known resonance method in X-band and the developed sensor. Measurement results demonstrate the robustness of this new sensor for characterizing rod shaped dielectric samples.

REFERENCES

[1] *Active Denial System*. Accessed: May 2021. [Online]. Available: https://en.wikipedia.org/wiki/Active_Denial_System
[2] J. Krupka, "Frequency domain complex permittivity measurements at microwave frequencies," *Meas. Sci. Technol.*, vol. 17, no. 6, pp. R55–R70, Jun. 2006.

[3] A. M. Nicolson and G. F. Ross, "Measurement of the intrinsic properties of materials by time-domain techniques," *IEEE Trans. Instrum. Meas.*, vol. IM-19, no. 4, pp. 377–382, Nov. 1970.
[4] W. B. Weir, "Automatic measurement of complex dielectric constant and permeability at microwave frequencies," *Proc. IEEE*, vol. 62, no. 1, pp. 33–36, Jan. 1974.
[5] J. Baker-Jarvis, E. J. Vanzura, and W. A. Kissick, "Improved technique for determining complex permittivity with the transmission/reflection method," *IEEE Trans. Microw. Theory Techn.*, vol. 38, pp. 1096–1103, Aug. 1990.
[6] J. R. Mosig, J.-C.-E. Besson, M. Gex-Fabry, and F. E. Gardiol, "Reflection of an open-ended coaxial line and application to nondestructive measurement of materials," *IEEE Trans. Instrum. Meas.*, vol. IM-30, no. 1, pp. 46–51, Mar. 1981.
[7] L. S. Anderson, G. B. Gajda, and S. S. Stuchly, "Analysis of an open-ended coaxial line sensor in layered dielectrics," *IEEE Trans. Instrum. Meas.*, vol. IM-35, no. 1, pp. 13–18, Mar. 1986.
[8] F. Horner, T. A. Taylor, R. Dunsmuir, J. Lamb, and W. Jackson, "Resonance methods of dielectric measurement at centimetre wavelengths," *J. Inst. Electr. Eng. III, Radio Commun. Eng.*, vol. 93, no. 21, pp. 53–68, Jan. 1946.
[9] U. Stumper, "A TE_{01n} cavity resonator method to determine the complex permittivity of low loss liquids at millimeter wavelengths," *Rev. Sci. Instrum.*, vol. 44, no. 2, pp. 165–169, Feb. 1973.
[10] J. Krupka and A. Milewski, "Accurate method of the measurement of complex permittivity of semiconductors in H_{01n} cylindrical cavity," *Electron. Technol.*, vol. 11, pp. 11–31, May 1978.
[11] B. W. Hakki and P. D. Coleman, "A dielectric resonator method of measuring inductive capacities in the millimeter range," *IRE Trans. Microw. Theory Techn.*, vol. 8, no. 4, pp. 402–410, Jul. 1960.
[12] W. E. Courtney, "Analysis and evaluation of a method of measuring the complex permittivity and permeability microwave insulators," *IEEE Trans. Microw. Theory Techn.*, vol. MTT-18, no. 8, pp. 476–485, Aug. 1970.
[13] J. Krupka, K. Derzakowski, B. Riddle, and J. Baker-Jarvis, "A dielectric resonator for measurements of complex permittivity of low loss dielectric materials as a function of temperature," *Meas. Sci. Technol.*, vol. 9, no. 10, pp. 1751–1756, Oct. 1998.
[14] R. N. Clarke and C. B. Rosenberg, "Fabry–Pérot and open resonators at microwave and millimeter wave frequencies, 2-300 GHz," *J. Phys. E, Sci. Instrum.*, vol. 15, no. 1, pp. 9–24, 1982.
[15] T. M. Hirvonen, P. Vainikainen, A. Lozowski, and A. V. Raisanen, "Measurement of dielectrics at 100 GHz with an open resonator connected to a network analyzer," *IEEE Trans. Instrum. Meas.*, vol. 45, no. 4, pp. 780–786, Aug. 1996.
[16] I. Danilov and R. Heidinger, "New approach for open resonator analysis for dielectric measurements at mm-wavelengths," *J. Eur. Ceram. Soc.*, vol. 23, no. 14, pp. 2623–2626, Jan. 2003.
[17] H. Y. Yao, J. Y. Jiang, Y. S. Cheng, Z. Y. Chen, T. H. Her, and T. H. Chang, "Modal analysis and efficient coupling of TE_{01} mode in small-core THz Bragg fibers," *Optic Exp.*, vol. 23, no. 21, pp. 27266–27281, 2015.
[18] T. H. Chang, C. H. Li, C. N. Wu, and C. F. Yu, "Exciting circular TE_{mn} modes at low terahertz region," *Appl. Phys. Lett.*, vol. 93, no. 11, Sep. 2008, Art. no. 111503.
[19] V. Kesari, *Metal- and Dielectric-Loaded Waveguide: An Artificial Material for Tailoring the Waveguide Propagation Characteristics*. London, U.K.: IntechOpen, Jan. 2019.
[20] J. Krupka, S. A. Gabelich, K. Derzakowski, and B. M. Pierce, "Comparison of split post dielectric resonator and ferrite disc resonator techniques for microwave permittivity measurements of polycrystalline yttrium iron garnet," *Meas. Sci. Technol.*, vol. 10, no. 11, pp. 1004–1008, Nov. 1999.

YEVHEN YASHCHYSHYN (Senior Member, IEEE) received the M.E. degree from Lviv Polytechnic National University, Lviv, Ukraine, in 1979, the Ph.D. degree from Moscow Institute of Electronics and Mathematics, Moscow, Russia, in 1986, and the D.Sc. (Habilitation) degree from Warsaw University of Technology (WUT), Warsaw, Poland, in 2006.

In 2016, he was promoted to a Professor. Since 1999, he has been with the Institute of Radioelectronics and Multimedia Technology, WUT, where he is currently a Professor and the Deputy Director for Research. He has authored more than 250 technical articles and has authored or coauthored five books. He holds several patents. His current research interests include antenna theory and techniques, smart beamforming, reconfigurable antennas, radio-over-fiber techniques, and materials characterization, including ferroelectric ceramic-polymers composites investigation up to subterahertz frequency. He was a recipient of the First Prize of EuMA at the 11th European Microwave Week for his outstanding research and new concept of the reconfigurable antenna, Amsterdam, The Netherlands, in 2008.

KRZYSZTOF DERZAKOWSKI was born in Minsk Mazowiecki, Poland, in 1959. He received the M.Sc. and Ph.D. degrees (Hons.) in electronic engineering from Warsaw University of Technology (WUT), Warsaw, Poland, in 1984 and 1991, respectively. Since 1985, he has been with the Institute of Radioelectronics and Multimedia Technology, WUT, where he is currently an Assistant Professor. He has authored or coauthored about 100 scientific articles in international journals and conference proceedings. His current research interests include measurements of dielectric and magnetic material properties at microwave frequencies, applications of dielectric resonators, EM field theory, and antenna techniques. He received the 1999 Best Paper Award in Measurements Science and Technology, U.K., and the First Prize of EuMA at the 11th European Microwave, Amsterdam, The Netherlands, in 2008.

CHANGYING WU (Member, IEEE) received the B.Eng. degree in electrical and electronic engineering, the M.Eng. degree in electromagnetic field and microwave technique, and the Ph.D. degree (Hons.) in circuit and system from Northwestern Polytechnical University, Xi'an, China, in 1999, 2001, and 2004, respectively.

He has been with the School of Electronics and Information, Northwestern Polytechnical University, since 2004, where he is currently an Associate Professor and the Head of the Department of Electronic Engineering. In 2011, he was a Visiting Scholar with the Radio Science Laboratory, Department of Electrical and Computer Engineering, The University of British Columbia, Canada. In 2015, he was a Visiting Scholar with the Department of Engineering and Digital Arts, University of Kent, U.K. His research interests include antenna design and microwave measurement.

GRZEGORZ CYWIŃSKI received the bachelor's and Master of Science degrees in microelectronics and semiconductor instruments from St. Petersburg Electrotechnical University, St. Petersburg, Russia, in 1995, the Ph.D. degree in physics in semiconductor physics from the Institute of Physics, Polish Academy of Sciences, Warsaw, Poland, in 2004, and the Habilitation degree in physics from the Institute of High Pressure Physics of the Polish Academy of Sciences (IHPP PAS), Warsaw, in 2020. Since September 2020, he has been the Scientific Affairs Director of the CENTERA Laboratories, IHPP PAS. He is the author or coauthor of more than 100 original articles in previewed scientific journals. His professional interests include semiconductor physics and technologies of devices based on tellurides, nitrides, and divers 2D materials. He is experienced in molecular beam epitaxy (tellurides, nitrides, and selenides), processing, technology, and applications of devices based on them. Recently, his scientific interests include novel designs and concepts of devices for high frequency research and their applications (including terahertz, subterahertz, and mm-waves ranges).